SWIFT-XRT-CALDB-06
Release Date: 2nd November 2005
Prepared by Joe Hill, Lorella Angelini and Alberto Moretti
Date Revised: 27th November 2006
Revision 4.0
Pages Changed: All.
Revision Note: This revision describes the derivation of a new boresight issued in a time-dependent TELDEF file (TELDEF 7), and a new boresight for the XRT onboard centroid calculation uploaded in November 2006.

SWIFT-XRT-CALDB-06: Boresight Analysis and Correction for the XRT

This document describes the calibration of the flight and ground software position accuracy for both Photon-Counting and Imaging modes. A new boresight has been determined and has been verified for all cases.

1. Boresight update motivation

In September 2006 the XRT team identified that the XRT position accuracy had decreased (Burrows et al., 2006); when considering the XRT positions of GRBs with optical counterparts, greater than 10% of the source positions quoted, were found to be outside of the associated 90% error circle. Several analyses were performed and it was determined that the boresight position had a time dependency and therefore CALDB required a time dependent TELDEF file. In addition, the XRT FSW required an updated boresight position. The results from the analysis are described in Section 3.

2. History

In January 2005, it was discovered that the spacecraft velocity aiding was effecting the XRT positions. This manifested itself as stellar aberration effects on the positions. Following the de-activation of the velocity aiding at 21:57 31st January 2005[1], additional calibrations of the XRT Image mode were performed on DOY 32, 33 and 34. Furthermore, analysis of these data led to updates of the flight centroiding parameters, which were verified against more calibration data obtained on DOY 60.

After the Flight Software (FSW) update to Build 8.9 on May 27th 2005, there was an event (possibly a micrometeroid impact), which damaged the CCD. Several columns had to be identified as hot pixels in the FSW. To quantify the effect on the centroiding algorithm onboard, and also to determine if the accuracy was affected, several observations of Cygnus X-3 and Cygnus X-1 were taken in Image mode on June 10th 2005.

[1] Data obtained prior to 21:57 31 January 2005 are corrected for stellar aberration effects in the SDC data processing.

During the first 6 months that *Swift* was on-orbit, there were several reports of position degradation with time, although these have never actually been quantified. Nevertheless, to ensure that the boresight calibration is valid for the entire duration on-orbit to November 2005, additional observations of Cygnus X-2 were obtained on 21st October 2005.

From comparing the XRT positions obtained from observations of calibration sources and GRBs with optical counterparts, it was determined that both the ground and the onboard default boresight needed to be calibrated and updated, see Figure 10. A new TELDEF (version 6) was issued in CALDB and a new boresight uploaded to the XRT in January 2006. This analysis is described in Section 4.

3. Boresight analysis (October 2006): TELDEF 7

3.1. Ground software boresight analysis

For a large sample of astronomical point-like sources (GRBs, Blazars, AGN, Neutron Stars listed in Table 5) observed between January 2006 and September 2006, we compared the cataloged optical positions to the XRT positions obtained from the *xrtpipeline* processing using version 6 of the TELDEF file in CALDB. We calculated the dependence of the sky-coordinate residuals (Optical RA/DEC - XRT RA/DEC) on the roll-angle of the observation. This allowed us to determine the amplitude and the direction of the mis-alignment of the telescope boresight.

From processing calibration data taken between January 2005 and October 2006 with the pre-launch TELDEF file (version 4) and plotting the residual off-set versus the date of the observation, it appears that the position accuracy is time dependent (Figure 1). Processing the same set of observations with the TELDEF version 6 (Figure 2) shows that the source positions obtained from observations prior to January 2006 have an improved and similar accuracy and that the positions calculated from observations obtained after January 2006 appear to be less accurate. A time dependent TELDEF file (version 7) has been derived such that the boresight corresponding to the epoch of the observation will be automatically used in the *xrtpipeline* processing. Processing the same set of observations (January 2005 – October 2006) with the time dependent TELDEF file (version 7), which has the boresight set to the value in TELDEF version 6 prior to January 2006 and the new boresight value for observations after January 2006, shows a consistent accuracy for all of the observations (Figure 3).

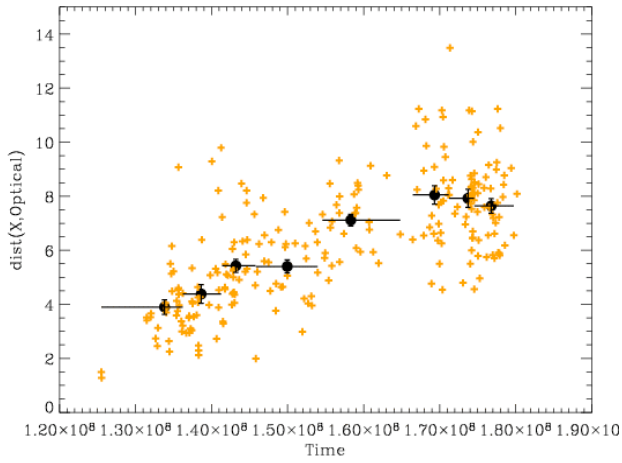

Figure 1. TELDEF 4: Pre-launch boresight applied to data from launch through September 2006. The x-axis is the time in seconds since 00:00.0 1 January 2001.

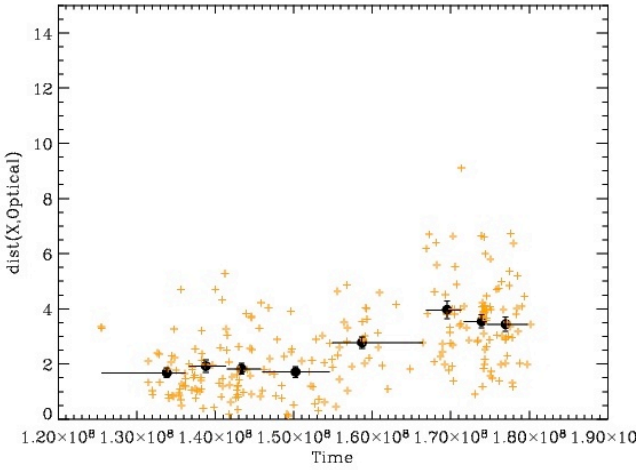

Figure 2. TELDEF 6: Update applied in January 2006 valid from launch applied to data from launch through September 2006. The x-axis is the time in seconds since 00:00.0 1 January 2001.

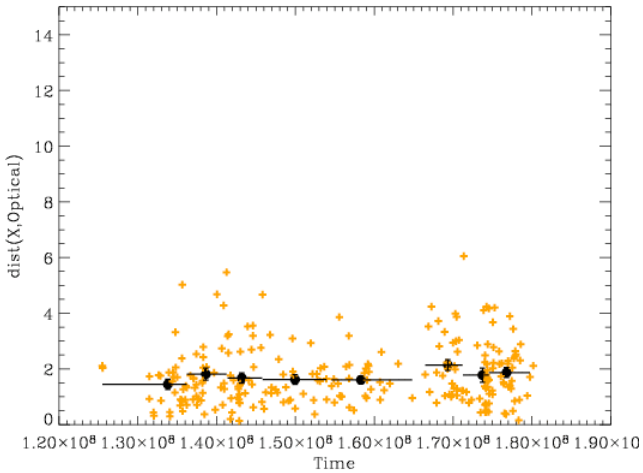

Figure 3. TELDEF 7: Time dependent boresight, i.e. prior to January 2006 the same boresight as TELDEF 6, after January 2006 the updated October 2006 boresight. The x-axis is the time in seconds since the 00:00.0 1 January 2001.

3.2. Image mode FSW boresight analysis

An *idl* script was used to recalculate the source position in the same way as the flight software but with the ability to input different boresight co-ordinates. The script reads in the data from the header of the telemetered postage stamp message obtained in Image mode. It then regenerates the centroid position in RA and DEC with or without the Telescope Alignment Monitor (TAM) correction (Hill et al. 2005). The script positions were compared with the onboard RA and DEC positions using the same boresight position to verify that the script calculation is identical to that performed by the onboard software. Varying the boresight used in the calculation allows an optimisation of the boresight definition to obtain the most accurate source positions.

Following the analysis of the ground processed calibration targets to determine the updated boresight position for CALDB TELDEF file, two sets of observations of Cyg X-1, Cyg X-2 and Cyg X-3 were obtained with the XRT operating in Image mode. The first set were obtained on the 31st October 2006 with the onboard boresight set to the January 2006 values (297.7 x 298.8) and the second set on 2nd November 2006 after uploading the new boresight value as derived for CALDB, but adjusted for the onboard co-ordinate system (296.7 x 298.0). The TDRSS postage stamps from the two observation sets are shown Figure 4 and Figure 5. The data for all three targets on both days were re-processed using the *idl* routine using the January 2006 boresight and the new boresight (Oct 06 from here forward).

The positions obtained by the flight software and from the *idl* routine relative to the known positions are shown in Figure 6 and Figure 7. Unfortunately the data obtained on the 31st October 2006 are less accurate in all cases due to the hot columns featuring more in these observations (Figure 4 compared to Figure 5) and decreasing the accuracy of the centroid position. Therefore only the observations obtained on 2nd November 2006 were used to verify the updated boresight. The position off-sets for the two boresights, shown in Figure 7, indicate that there is an improvement in accuracy by using the updated Oct 06 boresight compared to the Jan 06 value, although there appears that there is still some residual boresight off-set. Figure 8 shows the residual off-sets obtained from processing the Image mode data from 2nd November 2006 with the ground software and the TELDEF 7. The position accuracy is comparable with that of the flight software in Figure 7 (RHS).

To determine if the residual off-set was due to some continuing boresight drift with time, a predicted boresight was estimated from splitting the calibration data sample in section 3.1 into 4 mission epochs (DEC04, APR05, SEP05, JAN06, SEP06) and determining the best fit boresight position for each epoch. Plotting the boresight obtained for each epoch versus time (Figure 9, left) and extrapolating to the current time, one can obtain the boresight co-ordinate prediction for the current time. The boresight values used in CALDB are the average value for data obtained over the corresponding period of time. The boresight needed by the onboard software is the value valid at the current time. A predicted boresight of 296.3 x 297.3 was obtained. The *idl* script was applied to the 2nd November 2006 observations (Figure 9, right) but one can see that the residual off-sets are larger than those obtained with the Oct 06 boresight. The October 2006 value was loaded up to the onboard software on 24th November 2006 (Kennea et al., 2006).

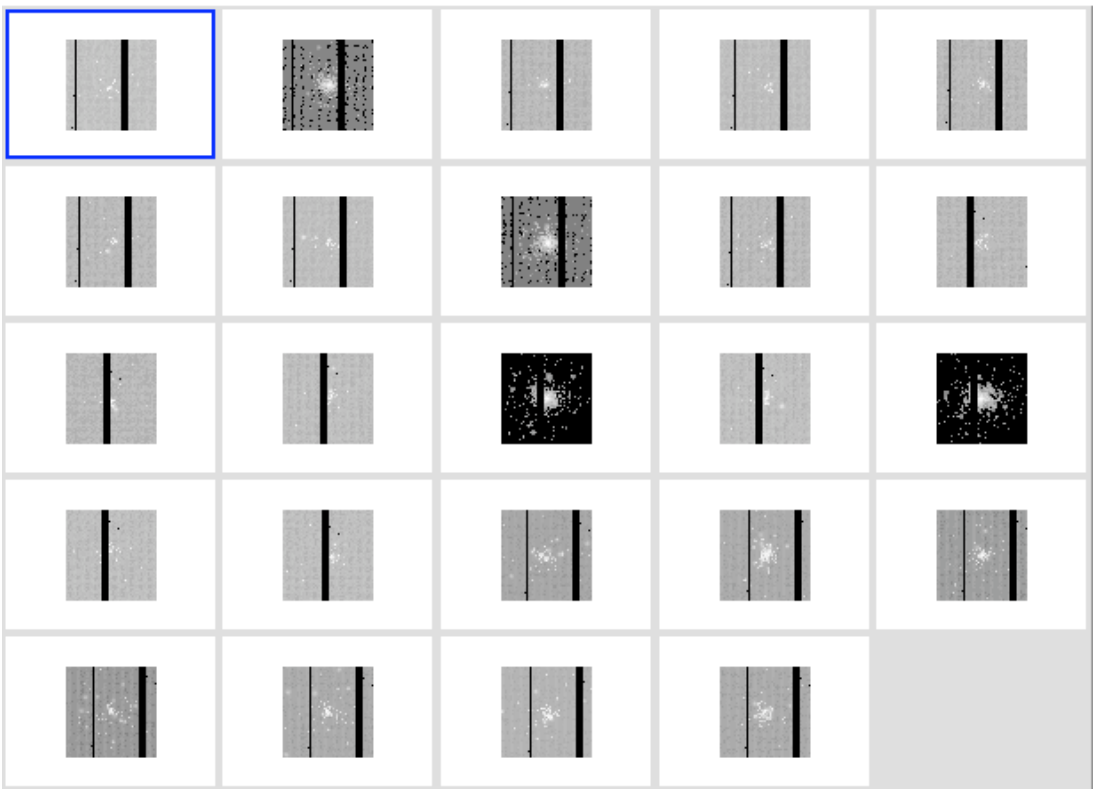

Figure 4 TDRSS Postage Stamp images obtained from the XRT FSW on 31st October 2006

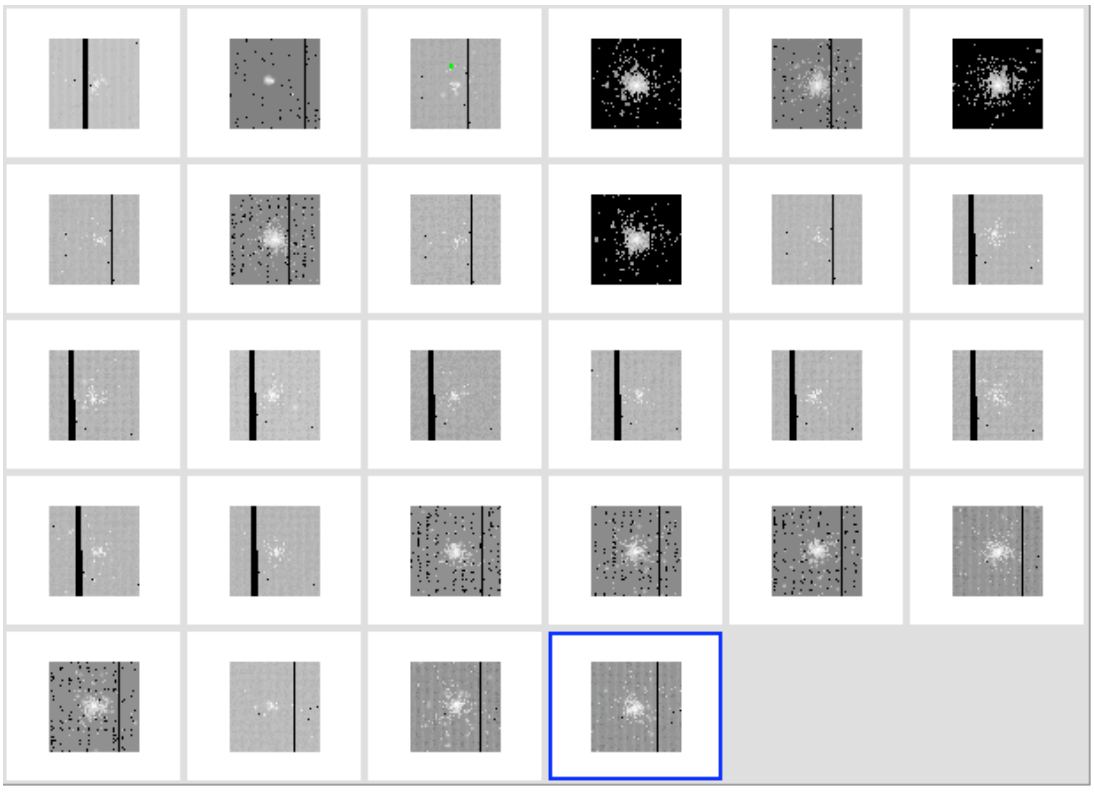

Figure 5 TDRSS Postage Stamp images obtained from the XRT FSW on 2nd November 2006

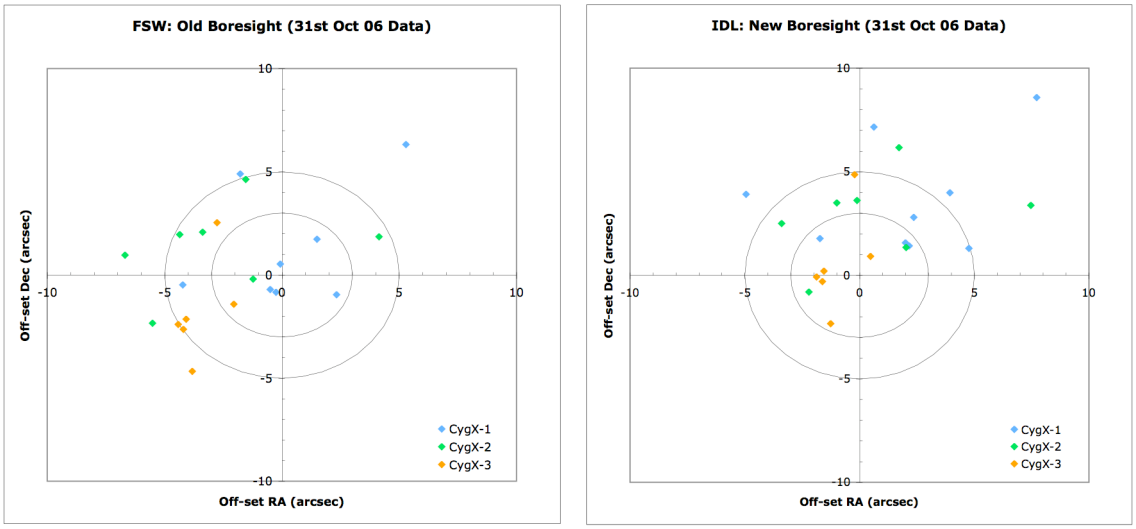

Figure 6. Position off-sets for the data obtained on the 31st October 2006. The off-sets shown are from using the onboard calculated positions and using the *idl* routine to recalculate the source position with alternate boresight positions and comparing with the known catalogued position.

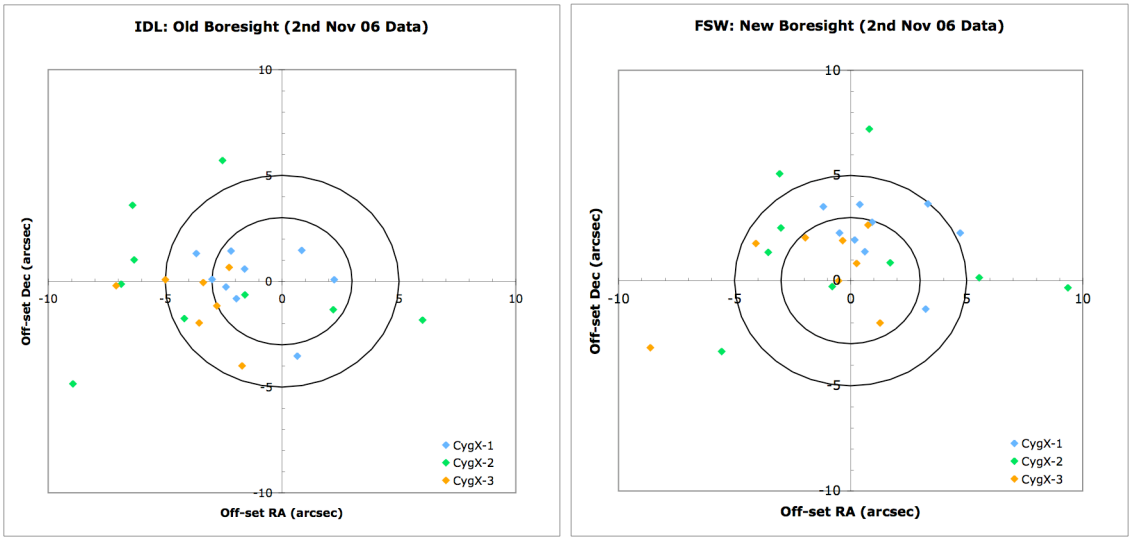

Figure 7 Position off-sets for the data obtained on the 2nd November 2006. The off-sets shown are from using the onboard calculated positions and using the *idl* routine to recalculate the source position with alternate boresight positions and comparing with the known catalogued position.

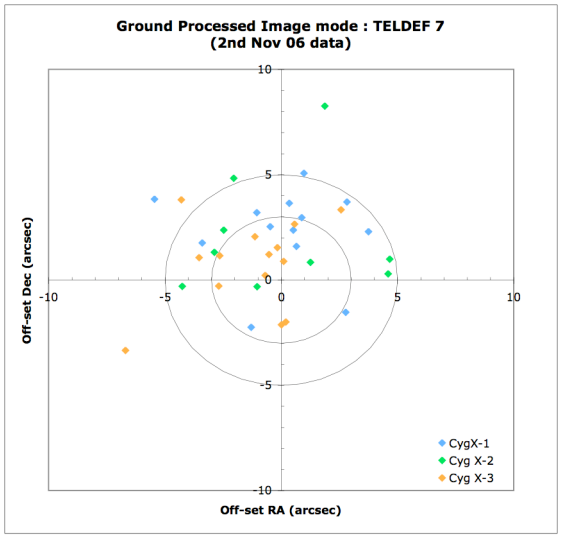

Figure 8. Position off-sets for the data obtained on the 2nd November 2006. The off-sets shown are from using the ground processed Image mode frames and TELDEF 7 to recalculate the source.

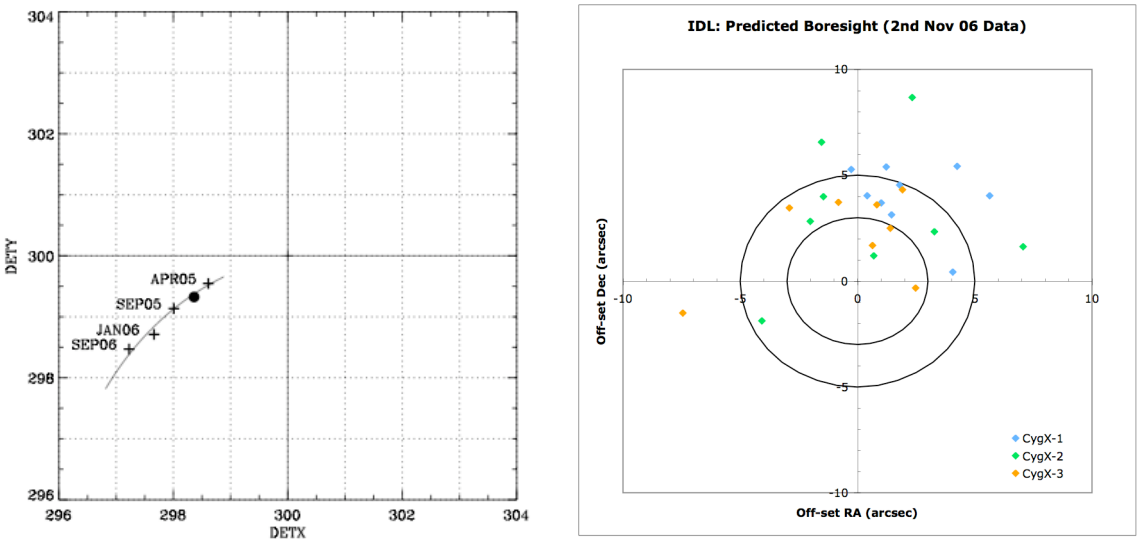

Figure 9. LHS: Best-fit boresight obtained for four mission epochs. RHS: Position off-sets using the extrapolated value for the boresight to process the 2nd November 2006 observations.

4. Boresight analysis (January 2005): TELDEF 6

4.1. Image mode boresight analysis

The *idl* script (described in Section 3) was run for a matrix of boresight positions for each Image mode observation of many calibration sources. A position off-set in RA and DEC was obtained for each observation by comparing the script position with the known optical position. From looking at the average off-set (optical – XRT) versus boresight position, one can determine the best-fit boresight co-ordinate. For data from the June 10th 2005 observations, the 21st October 2005 observations and the GRBs from launch through October 2005, the best-fit boresight was almost constant in the XRT x-axis. The majority of the variation from test-case to test-case was in the XRT y-axis. This analysis was performed for both TAM corrected and non-TAM corrected data.

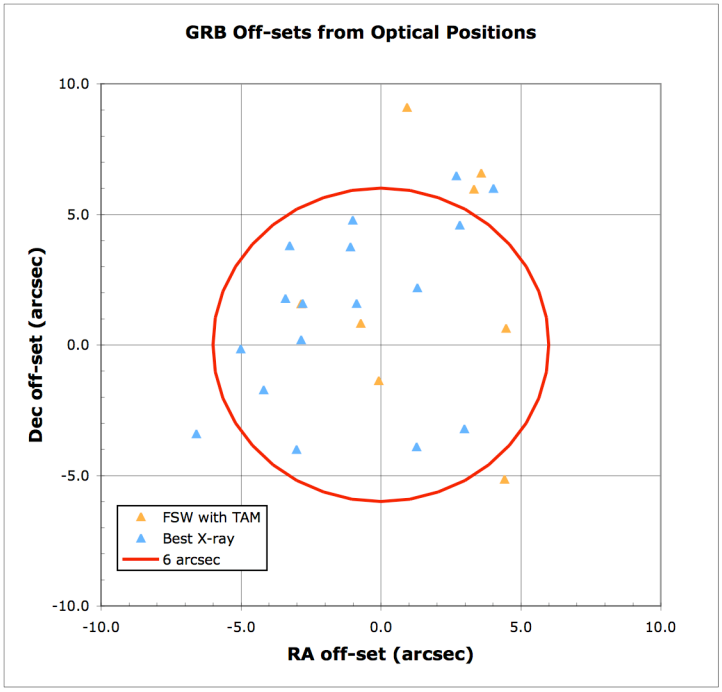

Figure 10. GRB off-sets from Optical positions with a default boresight position of 300x300 comparing the onboard FSW positions with the positions obtained from post-processing the event data on the ground.

4.2. Ground software boresight analysis

The best-fit boresight position obtained for Image mode was verified against Photon Counting (PC) mode data where the counting statistics are, in general, much improved. 11 sources and 36 observations were selected with a distribution of roll angles (Table 2). To limit the number of variables, this analysis was performed for data that were not corrected by the TAM.

Nine boresight positions were tested in a matrix around the best-fit Image mode boresight (Table 1). The different boresights were accounted for in the ground software TELDEF calibration file, by changing the offset in the detector coordinates. The data are shown in the Figure 11 for a subset of boresight positions. Additional verification was performed by

plotting the off-set in RA and Dec against the roll angle of the observation (see Figure 12), and verifying that there was no accuracy dependence on roll angle.

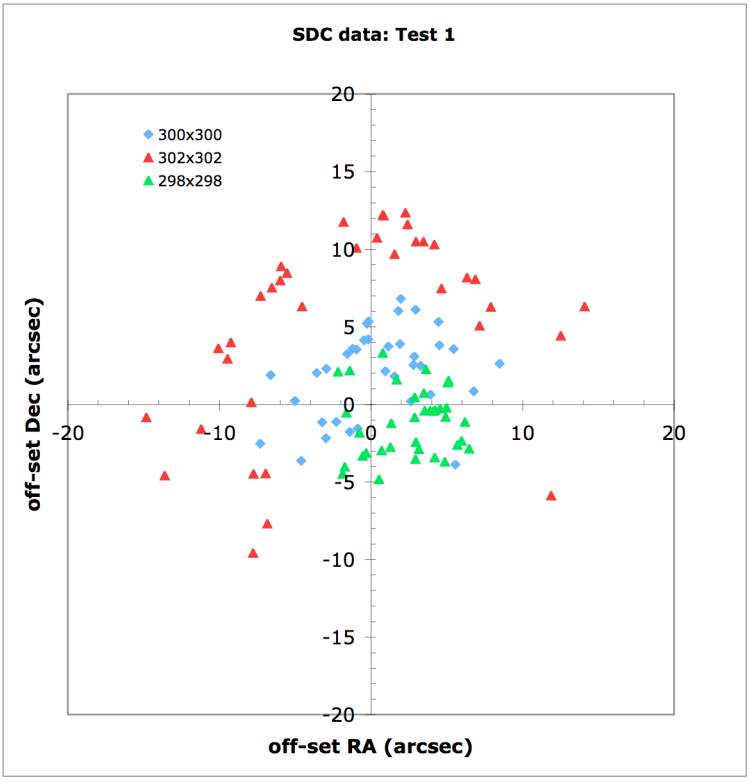

Figure 11. Variation of position off-sets for 36 observations of 11 sources with three boresight positions. Default at 300x300, best estimate from Image mode 298x298 and 302x302 for comparison.

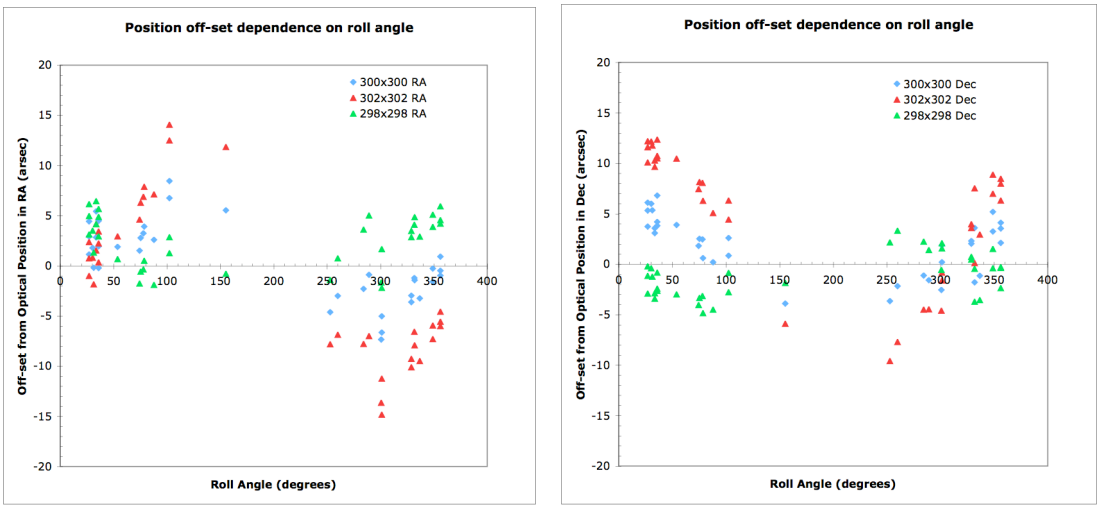

Figure 12. Variation of off-set in RA (left) and Dec (Right) with roll angle for different bore-sight positions; 300x300 (default), 298x298 (best-estimate Image mode) and 302x302 for comparison.

Table 1 The matrix of boresights analysed, showing the mean off-set for the calibration sources.

		X position				
		297	298	299	300	302
Y position	298		3.52		5.72	
	299	3.66	2.62	2.98		
	300		2.58		4.54	
	301		4.18			
	302					10.97
	Best Fit	298.2				
	299.3	2.26				

As in the Image mode analysis the average off-sets for each boresight position were plotted against the boresight y- and boresight x-position. From fitting a curve to the data, the boresight was further refined to 298.2 x 299.3 (Figure 13). This was confirmed as the best-fit position by reprocessing the observations with the refined boresight. The mean off-set for the default boresight decreased from 4.5'' to 2.1'' for the new boresight.

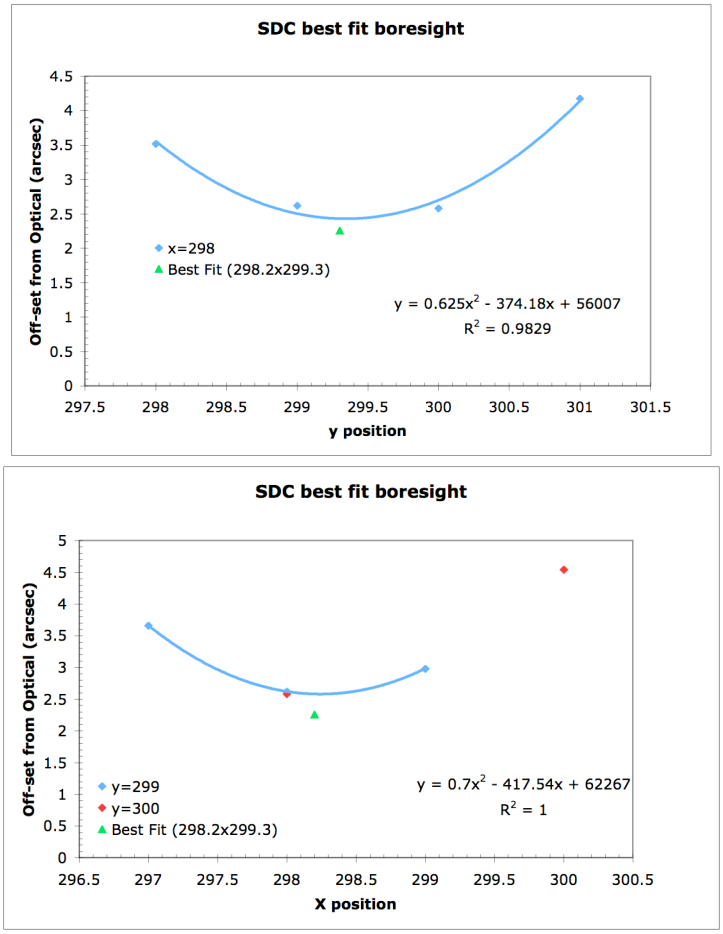

Figure 13. Polynomial fit to the average off-set from the optical position for 36 observations of 11 sources, for 10 boresight positions yielding a best-fit boresight position of 298.2x299.3.

Following the boresight optimisation, an additional 12 sources were analysed over 35 observations with the new boresight. The average off-set from the optical positions was found to be 2.21'' as seen in the previous sample, with 97% of the positions less than 5'' from the optical position. These data are shown in Figure 15.

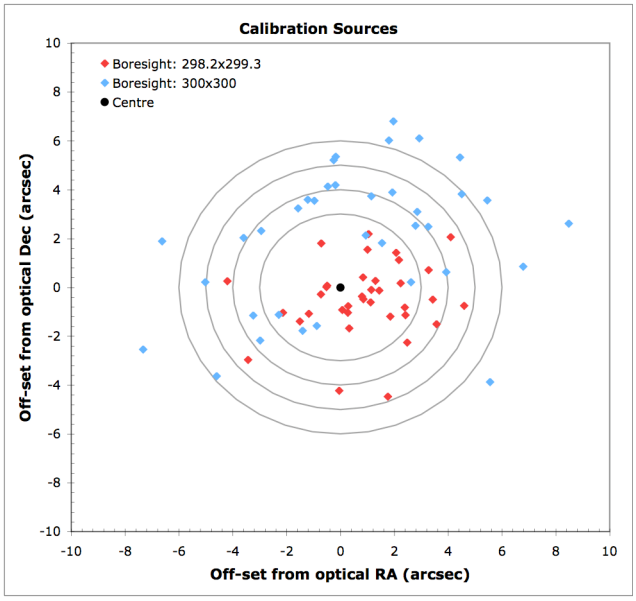

Figure 14. A comparison of calibration source position off-sets from optical positions for the default boresight and for a corrected boresight. The mean off-set for the boresight corrected positions is 2.3'' compared to 4.5'' for the default boresight.

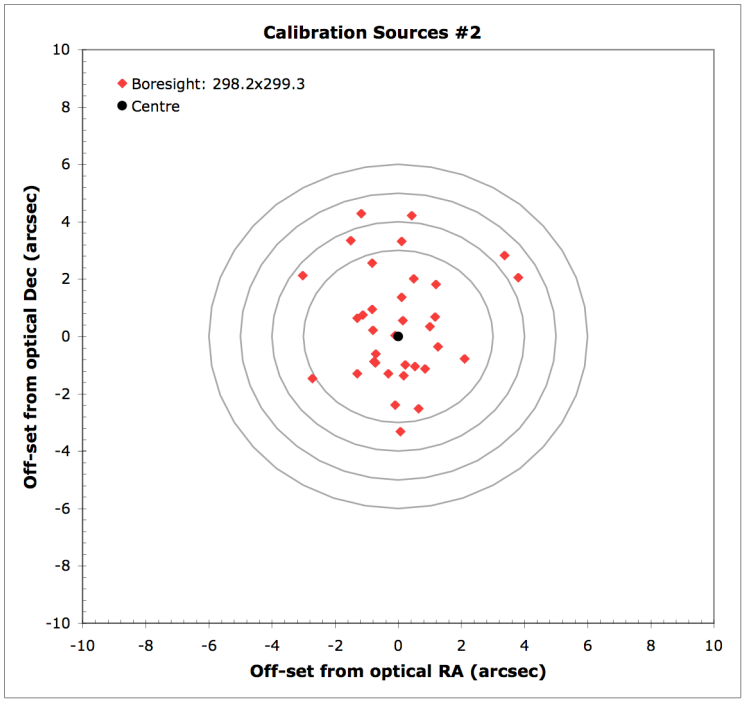

Figure 15. A comparison of additional calibration source position off-sets from optical positions for a corrected boresight. The mean off-set for the boresight corrected positions is 2.2''.

4.3. GRB analysis

A catalogue of 37 GRBs (Table 4) with optical counterparts observed between December 2004 and October 2005 were analysed with the default boresight (Figure 16) and the best-fit boresight position of 298.2 x 299.3 (Figure 17). The average distance from the optical counterpart of 2.3'' was confirmed to be the same as that obtained for the calibration sources.

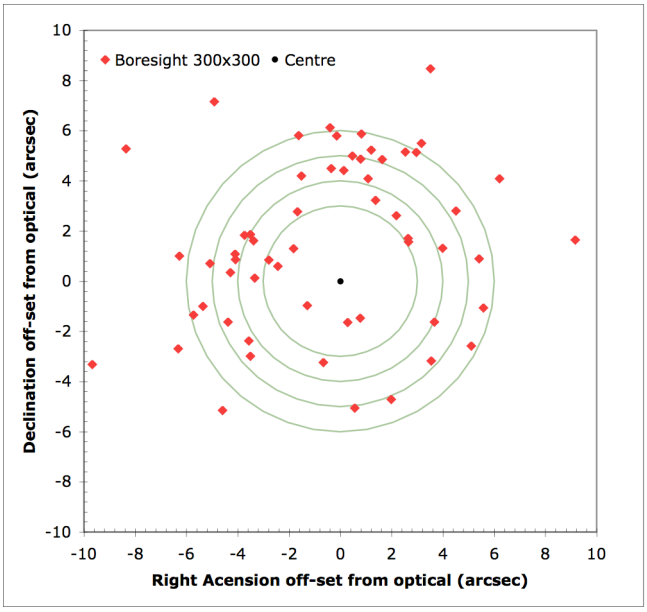

Figure 16. GRB position off-sets from optical positions for the default boresight.

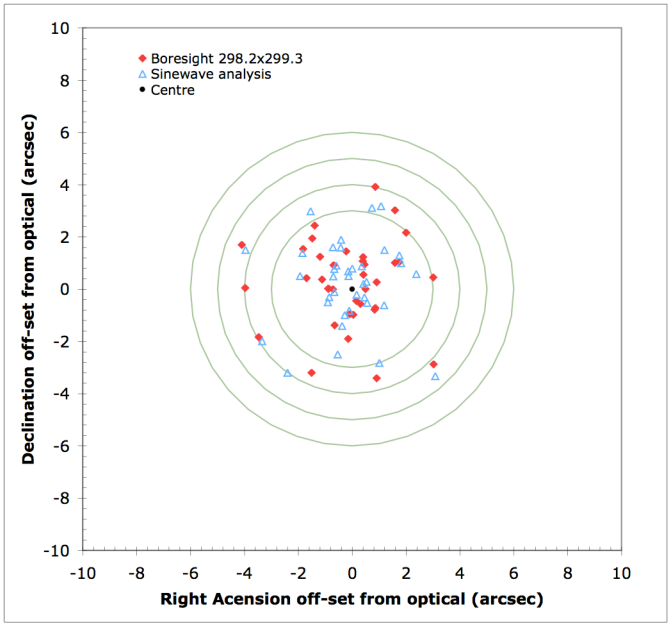

Figure 17. A Comparison of GRB position off-sets from optical positions for a sinewave corrected fit and using a corrected boresight.

A parallel analysis of the GRB positions was performed by plotting the RA and Dec off-sets relative to the optical counterpart against boresight and fitting a sinewave, the details are described in Morreti et al. We find that the implied boresight derived from the sinewave

analysis is consistent with the value obtained in this analysis. A plot of the position off-set of the GRBs from the optical counter-parts obtained by the two methods is shown in Figure 17.

In this analysis the TAM correction has not been applied. Preliminary results presented at the XRT Team Meeting in October (and in Hill et al.) using the default boresight (300 x 300), showed that the position accuracy was improved when the data were TAM corrected however, the positions show a residual off-set compared to those obtained with the new boresight. We find from preliminary analysis of the TAM correction with the new boresight, that the position accuracy is degraded. This is an indication that the TAM correction and the boresight position are not independent variables.

Calibration observations have been made in Image mode with the updated boresight position and confirm an improved FSW position accuracy.

4.4. Error analysis

A detailed error analysis has been performed and is documented in SWIFT-CALDB-07.

4.5. TELDEF updates

This best-fit boresight was implemented as an off-set in the TELDEF file (version 5) corresponding to a shift in the detector coordinates. In this way, the internal XRT detector coordinate system is no longer maintained. The algorithm used to derive the time of the events for the Timing modes uses the internal XRT detector coordinate system. The shift in the detector coordinates for the boresight correction introduces a small time shift (one row or less) to the Timing mode data. To maintain the XRT internal detector coordinate definition, the shift in the boresight can be included as a small misalignment in the matrix that translates the detector coordinates into sky coordinates. This change has been applied in version 6 of the TELDEF file. The two different TELDEFs (version 5 and 6) produce identical results when applied to data files derived with the same screening criteria and software release.

Table 2: Sources and observations selected for testing a matrix of different boresights to derive the best-fit boresight (January 2006). The table includes source name, sequence number, RA and Dec of the optical source position, start time of the observation, the roll angle and the XRT PC mode exposure.

Source name	Observation ID	Optical position: Right Ascension	Optical position: Declination	Start time (UTC)	Roll angle (degrees)	XRT exposure PC mode (Seconds)
NGC5548	30022004	14 17 59.65	+25 08 13.4	4/8/05 8:40	35.79522	440.41
NGC5548	30022005	14 17 59.65	+25 08 13.4	4/8/05 11:52	35.80822	242.24
NGC5548	30022006	14 17 59.65	+25 08 13.4	4/8/05 15:06	35.79035	277.52
NGC5548	30022014	14 17 59.65	+25 08 13.4	4/10/05 7:18	33.49466	1498.63
NGC5548	30022015	14 17 59.65	+25 08 13.4	4/9/05 18:31	33.49481	1307.12
NGC5548	30022033	14 17 59.65	+25 08 13.4	4/12/05 13:56	30.18841	317.15
NGC5548	30022040	14 17 59.65	+25 08 13.4	4/14/05 15:49	26.90384	287.19
NGC5548	30022045	14 17 59.65	+25 08 13.4	4/14/05 17:25	26.90242	292.18
NGC5548	30022046	14 17 59.65	+25 08 13.4	4/14/05 19:03	26.89817	292.18
NGC5548	30022048	14 17 59.65	+25 08 13.4	4/26/05 9:52	356.10055	220.62
NGC5548	30022047	14 17 59.65	+25 08 13.4	4/26/05 10:56	356.09505	1030.48
NGC5548	30022049	14 17 59.65	+25 08 13.4	4/26/05 12:35	356.08969	1043.02
NGC5548	30022054	14 17 59.65	+25 08 13.4	5/10/05 17:07	348.78813	1055.57
NGC5548	30022055	14 17 59.65	+25 08 13.4	5/10/05 19:00	348.78329	814.86
QSO J2253+1608	30024001	22 53 57.75	+16 08 53.56	5/11/05 14:41	77.86438	1426.63
QSO J2253+1608	30024002	22 53 57.75	+16 08 53.56	5/19/05 12:36	74.28865	4522.92
OJ287	35011001	08 54 48.87	+20 06 30.64	5/20/05 5:14	289.01704	3715.63
OJ287	35011003	08 54 48.87	+20 06 30.64	6/7/05 13:35	284.16883	1253.64
Mkn421	35014002	11 04 27.31	+38 12 31.80	4/1/05 4:08	331.8063	385.31
Mkn180	35015001	11 36 26.41	+70 09 27.3	4/16/05 0:24	328.73897	2943.45
Mkn180	35015002	11 36 26.41	+70 09 27.3	4/18/05 3:23	328.73572	6398.48
Mkn501	35023001	16 53 52.22	+39 45 36.61	4/21/05 1:01	53.75609	546.56
Mkn501	35023002	16 53 52.22	+39 45 36.61	6/17/05 22:41	351.66501	1835.32
BLLac	35028001	22 02 43.29	+42 16 39.98	7/25/05 22:08	31.27963	566.51
3C454.3	35030001	22 53 57.75	+16 08 53.56	4/24/05 18:38	87.84266	13724.1
3C454.3	35030003	22 53 57.75	+16 08 53.56	5/17/05 16:18	75.2958	4771.34
AKN564	35062001	22 42 39.47	+29 43 30.0	4/19/05 15:28	102.32689	4605.84
AKN564	35062256	22 42 39.47	+29 43 30.0	4/27/05 0:39	102.29757	4675.91
AKN564	35062002	22 42 39.47	+29 43 30.0	5/19/05 0:22	78.56376	4410.25
Mkn684	35078001	14 31 04.7	+28 17 13	7/14/05 9:48	301.20647	4758.83
Mkn684	35078002	14 31 04.7	+28 17 13	7/14/05 9:28	301.19094	386.09
Mkn684	35078004	14 31 04.7	+28 17 13	7/15/05 5:06	300.5782	589.18
Mkn684	35078006	14 31 04.7	+28 17 13	9/15/05 0:39	259.77146	12907.5
Mkn684	35078007	14 31 04.7	+28 17 13	9/18/05 2:52	252.72212	8226.22
Mkn421	52100009	11 04 27.31	+38 12 31.80	10/4/05 4:19	155.17124	8048.35
Mkn813	56600002	14 27 25.06	+19 49 51.5	5/20/05 10:57	336.63431	707.03

Table 3: Sources and observations selected as control sample for the best-fit boresight position (January 2006). The table includes source name, sequence number, RA and Dec of the optical source position, start time of the observation and the XRT PC mode exposure.

Source name	Observation ID	Optical position: Right Ascension	Optical position: Declination	Start time (UTC)	Roll angle (degrees)	XRT exposure PC mode (Seconds)
PKS0537-441	30138001	05 38 50.36	-44 05 08.939	7/12/05 0:02	27.14861	4978.46
1ES0120+340	35000001	01 23 08.90	+34 20 50	6/9/05 16:57	78.77028	1607.15
PKS0208-512	35002001	02 10 46.20	-51 01 01.89	4/22/05 23:43	359.884	12300.7
PKS0208-512	35002003	02 10 46.20	-51 01 01.89	5/5/05	10.71307	2030.87
PKS0208-512	35002004	02 10 46.20	-51 01 01.89	5/12/05 0:19	17.25286	2108.62
PKS0208-512	35002005	02 10 46.20	-51 01 01.89	5/10/05 0:15	15.41735	4114.37
3C66A	35003001	02 22 39.61	+43 02 07.80	6/29/05 10:56	89.80221	5025.83
1H0323+022	35006001	03 26 13.97	+02 25 14.70	6/26/05 13:15	59.91305	10741.1
1H0323+022	35006002	03 26 13.97	+02 25 14.7	6/29/05 17:26	61.34463	4676.07
1H0323+022	35006003	03 26 13.97	+02 25 14.7	7/11/05 2:51	65.42399	6586.64
1ES1011+496	35012002	10 15 04.17	+49 26 00.6	6/19/05 19:17	267.536	7998.24
1ES1011+496	35012003	10 15 04.17	+49 26 00.6	6/26/05 7:14	262.2681	9157.33
1H1100-230	35013001	11 03 37.57	-23 29 30.2	6/30/05 0:06	300.8013	8554.73
1ES2344+514	35031002	23 47 04.92	+51 42 17.9	5/19/05 16:09	101.353	4199.69
1H1426+428	35020003	14 28 32.50	+42 40 25	4/2/05 17:59	32.42575	1293.879
H1426+428	51000002	14 28 32.50	+42 40 25	6/19/05 4:56	319.449	21462.5
H1426+428	51000003	14 28 32.50	+42 40 25	6/25/05 5:54	314.8236	22908.6
1ES2344+514	35031001	23 47 04.92	+51 42 17.9	4/19/05 0:30	136.6156	4683.53
1ES2344+514	35031002	23 47 04.92	+51 42 17.9	5/19/05 16:09	101.3537	4199.69
PKS0823-223	35071001	08 26 01.57	-22 30 27.20	6/20/05 23:51	320.5244	2908.4
PKS0823-223	35071002	08 26 01.57	-22 30 27.20	7/1/05 0:10	329.8242	20367.9
PKS0823-223	35071003	08 26 01.57	-22 30 27.20	7/3/05 0:19	332.4729	31355.1
PKS0823-223	35071004	08 26 01.57	-22 30 27.20	9/6/05 3:41	57.23821	7376.38
PKS0823-223	35071005	08 26 01.57	-22 30 27.20	9/22/05 20:39	82.62095	5106.88
PKS0823-223	35071006	08 26 01.57	-22 30 27.20	9/28/05 9:11	85.8729	5887.07
PKS0823-223	35071007	08 26 01.57	-22 30 27.20	9/28/05 18:45	87.0129	8938.38
PKS0823-223	35071008	08 26 01.57	-22 30 27.20	9/29/05 18:27	86.41886	16161.8
PKS0823-223	35071009	08 26 01.57	-22 30 27.20	10/2/05 7:05	90.11244	12395.4
RXJ0148.3-2758	35075002	01 48 22.33	-27 58 25.7	5/5/05 23:59	22.16315	7742.409
RXJ0148.3-2758	35075003	01 48 22.33	-27 58 25.7	5/7/05 0:00	24.21947	22128.31
RXJ0148.3-2758	35075004	01 48 22.33	-27 58 25.7	5/11/05 0:26	27.13348	8875.74
RXJ0148.3-2758	35075006	01 48 22.33	-27 58 25.7	5/13/05 0:18	29.059	3144.09
Mkn728	35168001	11 01 01.77	+11 02 48.3	7/14/05 1:32	290.9755	4488.03
Mkn728	35168003	11 01 01.77	+11 02 48.3	10/24/05 20:51	105.8357	6561.35
Mkn915	35169001	22 36 46.50	-12 32 42.6	7/10/05 23:31	78.29587	2938.509

Table 4: GRBs with confirmed optical counterparts used for the boresight analysis (January 2006).

GRB Name	Observation ID	RA of optical counterpart	Dec of optical counterpart
GRB 041223	100585001	100.1971	-37.0729
GRB 050126	103780000	278.1132	42.3704
GRB 050219b	106442000	81.3166	-57.7580
GRB 050315	111063000	306.4754	-42.6006
GRB 050318	111529000	49.7125	-46.3956
GRB 050319	111622000	154.1996	43.5485
GRB 050401	113120000	247.8700	2.1873
GRB 050406	113872000	34.4679	-50.1875
GRB 050408	20004001	180.5722	10.8528
GRB 050412	114485000	181.1044	-1.2010
GRB 050416a	114753000	188.4775	21.0574
GRB 050502b	116116000	142.5418	16.9967
GRB 050505	117504000	141.7638	30.2733
GRB 050509a	118707000	310.5817	54.0716
GRB 050525	130088000	278.1358	26.3399
GRB 050603	131560001	39.9868	-25.1819
GRB 050607	132247000	300.1783	9.1421
GRB 050712	145581000	77.7004	64.9132
GRB 050713a	145675000	320.5400	77.0747
GRB 050714b	145994000	169.6988	-15.5477
GRB 050716	146227000	338.5864	38.6843
GRB 050721	146970000	253.4355	-28.3811
GRB 050724	147478000	246.1849	-27.5410
GRB 050726	147788000	200.0496	-32.0644
GRB 050730	148225000	212.0714	-3.7716
GRB 050801	148522000	204.1475	-21.9283
GRB 050802	148646000	219.2737	27.7867
GRB 050814	150314000	264.1891	46.3393
GRB 050815	150532000	293.5965	9.1465
GRB 050820a	151207000	337.4088	19.5603
GRB 050824	151905001	12.2338	22.6089
GRB 050826	152113000	87.7566	-2.6432
GRB 050904	153514000	13.7117	14.0861
GRB 050908	154112000	20.4613	-12.9544
GRB 050915a	155242000	81.6868	-28.0165
GRB 050922c	156467000	317.3879	-8.7583
GRB051016b	159994000	132.1159	13.6556

Table 5: Calibration sources and GRBs with confirmed optical counterparts used for the October 2006 boresight analysis.

Name	RA Optical	Dec Optical	RA XRT	DEC XRT	error	Delta RA	Delta DEC	Roll	Counts	Exposure
GRB050408	180.5722	10.8528	180.5733	10.8518	3.59	-1.20	-1.03	324.2	908	10106.7
GRB060121	137.4664	45.6626	137.4675	45.6612	3.73	-0.85	-1.25	9.7	335	4935.2
NGC5548	214.4985	25.1371	214.4977	25.1361	4.03	-0.50	-0.41	35.8	135	439.0
NGC5548	214.4985	25.1371	214.4977	25.1361	3.64	-1.02	-1.06	33.5	572	1496.6
NGC5548	214.4985	25.1371	214.4972	25.1358	3.67	-1.06	-1.17	33.5	457	1306.2
NGC5548	214.4985	25.1371	214.4978	25.1358	3.96	-0.98	-0.87	30.2	154	317.2
NGC5548	214.4985	25.1371	214.4980	25.1356	4.06	-0.70	-0.05	26.9	131	286.2
NGC5548	214.4985	25.1371	214.4978	25.1360	4.00	-1.33	-0.83	26.9	148	291.8
NGC5548	214.4985	25.1371	214.4972	25.1357	4.09	-1.20	-1.47	26.9	119	290.6
NGC5548	214.4985	25.1371	214.4989	25.1359	3.67	-0.85	-1.11	356.1	488	1028.7
NGC5548	214.4985	25.1371	214.4985	25.1364	4.21	-0.74	-1.65	356.1	101	218.8
NGC5548	214.4985	25.1371	214.4988	25.1362	3.66	-0.85	-0.82	356.1	523	1041.4
NGC5548	214.4985	25.1371	214.4990	25.1360	3.64	-0.75	-1.12	348.8	569	1055.6
NGC5548	214.4985	25.1371	214.4987	25.1356	3.68	-0.89	-1.24	348.8	442	814.2
SAXJ1808.4-3658	272.1148	-36.9790	272.1146	-36.9782	3.53	-1.22	-0.10	162.9	2499	787.3
SAXJ1808.4-3658	272.1148	-36.9790	272.1182	-36.9771	7.97	-0.78	-2.19	258.4	6	1040.5
SAXJ1808.4-3658	272.1148	-36.9790	272.1165	-36.9775	3.52	-0.94	-1.10	261.2	3437	2343.9
SAXJ1808.4-3658	272.1148	-36.9790	272.1172	-36.9770	6.12	-1.48	0.27	266.6	13	1674.9
SAXJ1808.4-3658	272.1148	-36.9790	272.1163	-36.9780	3.54	-0.82	-0.90	266.5	2266	1928.0
SAXJ1808.4-3658	272.1148	-36.9790	272.1161	-36.9776	4.15	0.63	-0.97	266.5	98	2549.9
SAXJ1808.4-3658	272.1148	-36.9790	272.1155	-36.9774	5.64	-1.14	-1.24	266.5	23	2836.3
SAXJ1808.4-3658	272.1148	-36.9790	272.1168	-36.9769	5.31	-1.38	-3.76	261.1	13	9009.8
SAXJ1808.4-3658	272.1148	-36.9790	272.1169	-36.9773	4.64	-0.58	-1.34	264.2	42	7328.6
SAXJ1808.4-3658	272.1148	-36.9790	272.1171	-36.9765	6.04	-3.48	-4.02	267.2	12	2985.6
SAXJ1808.4-3658	272.1148	-36.9790	272.1177	-36.9776	5.44	0.75	-0.08	265.0	13	7756.3
SAXJ1808.4-3658	272.1148	-36.9790	272.1172	-36.9773	5.31	-1.58	-1.77	265.6	12	6742.1
SAXJ1808.4-3658	272.1148	-36.9790	272.1186	-36.9798	6.93	-0.46	2.39	265.4	6	4736.3
UGC01928	37.0467	43.8524	37.0382	43.8520	4.59	-10.10	-0.89	100.0	6	18444.5
4U0142+61	26.5934	61.7509	26.5910	61.7500	3.51	-1.05	-0.86	82.8	13935	7430.5
PKS0537-441	84.7098	-44.0858	84.7095	-44.0870	3.60	-0.84	-0.78	27.1	886	4977.2
PKS0537-441	84.7098	-44.0858	84.7076	-44.0851	3.67	-0.78	-0.93	154.3	469	6373.5
PKS0537-441	84.7098	-44.0858	84.7079	-44.0844	3.66	-0.69	-0.70	162.9	495	6243.1
RSOph	267.5550	-6.7079	267.5533	-6.7098	3.52	-1.28	-1.07	67.4	3993	1815.3
RSOph	267.5550	-6.7079	267.5536	-6.7097	3.53	-0.99	-1.18	65.0	3220	2108.7
RSOph	267.5550	-6.7079	267.5542	-6.7099	3.56	-1.02	-0.96	44.3	1293	1647.3
RSOph	267.5550	-6.7079	267.5544	-6.7097	3.58	-0.91	-1.16	40.0	994	1767.6
RSOph	267.5550	-6.7079	267.5543	-6.7104	3.66	-1.23	-0.91	31.3	480	1587.1
RSOph	267.5550	-6.7079	267.5543	-6.7101	3.63	-1.14	-0.66	40.3	614	2327.0
RSOph	267.5550	-6.7079	267.5552	-6.7103	3.61	-0.74	-1.29	22.7	750	3577.9
RSOph	267.5550	-6.7079	267.5567	-6.7092	3.74	-1.28	-1.04	329.8	328	2073.5
RSOph	267.5550	-6.7079	267.5563	-6.7080	3.64	-1.06	-0.95	305.0	586	4455.3
RSOph	267.5550	-6.7079	267.5565	-6.7082	3.74	-0.52	-1.00	307.6	328	2855.7
RSOph	267.5550	-6.7079	267.5563	-6.7084	3.71	-1.27	-0.91	293.7	361	4658.5
RSOph	267.5550	-6.7079	267.5567	-6.7077	4.61	-0.98	-0.85	274.1	60	905.1
RSOph	267.5550	-6.7079	267.5565	-6.7073	3.68	-1.89	-0.86	270.4	386	10462.9
RSOph	267.5550	-6.7079	267.5564	-6.7071	3.81	-0.80	-1.17	276.4	244	4333.9
RSOph	267.5550	-6.7079	267.5570	-6.7070	3.71	-0.61	-0.68	262.8	374	7526.8
BLLac	330.6804	42.2778	330.6791	42.2758	3.58	-1.00	-1.05	63.9	1026	4515.6
BLLac	330.6804	42.2778	330.6784	42.2759	3.58	-1.23	-1.04	65.1	1048	3940.8
Mkn501	253.4676	39.7602	253.4698	39.7591	3.51	-1.06	-0.99	325.8	7389	4483.0
Mkn501	253.4676	39.7602	253.4710	39.7591	3.54	-2.31	-1.51	307.1	1612	997.9
Mkn501	253.4676	39.7602	253.4696	39.7599	3.54	-1.14	-1.24	308.6	1819	1028.0
Mkn501	253.4676	39.7602	253.4704	39.7592	3.51	-0.65	-1.27	311.1	6462	2965.9
Mkn501	253.4676	39.7602	253.4697	39.7594	3.52	-0.86	-0.65	307.8	4259	2287.4
PKS2155-304	329.7170	-30.2256	329.7143	-30.2256	3.55	-0.95	-1.96	139.6	1515	762.2
PKS2155-304	329.7170	-30.2256	329.7142	-30.2251	3.52	-0.87	-1.09	145.3	3505	1243.6
PKS2155-304	329.7170	-30.2256	329.7154	-30.2248	3.55	-0.70	-0.87	148.6	1329	556.6
PKS2155-304	329.7170	-30.2256	329.7142	-30.2248	3.54	-0.77	-0.63	146.0	1678	682.0
PKS2155-304	329.7170	-30.2256	329.7151	-30.2242	3.55	-1.85	1.78	161.9	1392	651.3
PKS2155-304	329.7170	-30.2256	329.7149	-30.2241	3.54	-1.65	-1.60	164.2	1603	682.0
PKS2155-304	329.7170	-30.2256	329.7150	-30.2245	3.55	-1.04	-0.74	162.5	1468	782.3
PKS2155-304	329.7170	-30.2256	329.7152	-30.2258	3.54	-1.47	-0.54	139.7	1730	1135.8
PKS2155-304	329.7170	-30.2256	329.7148	-30.2254	3.55	-1.05	-1.11	126.0	1667	935.2
PKS2155-304	329.7170	-30.2256	329.7151	-30.2245	3.56	-0.75	-1.08	161.0	1333	902.6
PKS2155-304	329.7170	-30.2256	329.7141	-30.2254	3.58	-1.70	-1.46	135.0	963	946.8

Name	RA Optical	Dec Optical	RA XRT	DEC XRT	error	Delta RA	Delta DEC	Roll	Counts	Exposure
PKS2155-304	329.7170	-30.2256	329.7140	-30.2254	3.56	-0.76	-1.18	136.5	1370	1010.4
PKS2155-304	329.7170	-30.2256	329.7158	-30.2237	3.54	-1.21	-1.05	180.8	1842	1120.8
PKS2155-304	329.7170	-30.2256	329.7170	-30.2225	3.64	-0.72	-0.73	205.5	499	406.2
PKS2155-304	329.7170	-30.2256	329.7168	-30.2236	3.68	-0.45	-0.92	208.8	386	250.7
PKS2155-304	329.7170	-30.2256	329.7173	-30.2240	3.59	-0.56	-1.21	211.2	870	390.8
PKS2155-304	329.7170	-30.2256	329.7168	-30.2227	3.63	-0.34	-0.51	214.3	566	401.7
PKS2155-304	329.7170	-30.2256	329.7173	-30.2234	3.58	-0.69	-0.72	219.6	1049	907.6
PKS2155-304	329.7170	-30.2256	329.7177	-30.2233	3.56	-1.01	-1.08	222.9	1233	947.4
PKS2155-304	329.7170	-30.2256	329.7168	-30.2232	3.57	-1.09	-0.50	223.9	1091	621.8
PKS2155-304	329.7170	-30.2256	329.7168	-30.2239	3.59	-1.48	-0.85	224.4	858	519.0
1ES0120+340	20.7871	34.3472	20.7844	34.3459	3.57	-1.52	-0.67	78.8	1103	1607.1
1ES0120+340	20.7871	34.3472	20.7843	34.3451	3.53	-0.88	-0.91	65.2	3030	5460.8
1ES0120+340	20.7871	34.3472	20.7843	34.3452	3.57	-0.80	-1.32	64.4	1172	2462.1
PKS0208-512	32.6925	-51.0172	32.6931	-51.0181	3.59	-1.04	-0.99	359.9	901	12300.1
PKS0208-512	32.6925	-51.0172	32.6946	-51.0177	6.93	0.50	-1.30	334.9	11	212.3
PKS0208-512	32.6925	-51.0172	32.6929	-51.0181	3.95	-1.19	-1.14	10.7	157	2028.5
PKS0208-512	32.6925	-51.0172	32.6929	-51.0183	4.00	-1.35	-0.83	17.3	140	2108.6
PKS0208-512	32.6925	-51.0172	32.6928	-51.0180	3.79	-0.89	-1.68	15.4	262	4114.4
3C66A	35.6651	43.0355	35.6634	43.0350	3.65	-1.13	-1.02	89.8	543	5025.8
3C66A	35.6651	43.0355	35.6672	43.0353	3.51	-1.11	-1.30	318.0	6731	51876.0
1H0323+022	51.5582	2.4208	51.5573	2.4206	3.62	-0.55	-1.00	59.9	689	10738.6
1H0323+022	51.5582	2.4208	51.5578	2.4195	3.79	-1.03	-0.86	61.3	243	4674.2
1H0323+022	51.5582	2.4208	51.5569	2.4197	3.78	-0.84	-1.05	65.4	270	6586.6
OJ287	133.7037	20.1085	133.7042	20.1088	3.82	-1.35	-1.26	289.0	241	3715.6
OJ287	133.7037	20.1085	133.7044	20.1090	4.09	-0.94	-0.71	284.2	127	1253.6
1ES1011+496	153.7674	49.4335	153.7686	49.4342	3.52	-1.18	-1.03	267.5	4800	7998.2
1ES1011+496	153.7674	49.4335	153.7681	49.4343	3.51	-1.03	-0.92	262.3	6205	9157.3
1ES1011+496	153.7674	49.4335	153.7644	49.4318	3.51	-1.22	-0.86	77.2	5729	7674.6
1H1100-230	165.9065	-23.4917	165.9081	-23.4921	3.51	-1.16	-0.84	300.8	13138	8554.7
1H1100-230	165.9065	-23.4917	165.9084	-23.4922	3.52	-1.01	-0.82	307.4	3678	2304.2
1H1100-230	165.9065	-23.4917	165.9046	-23.4925	3.57	-1.79	-1.23	100.6	1017	1168.0
1H1100-230	165.9065	-23.4917	165.9051	-23.4930	3.61	-0.91	-0.95	87.9	683	556.6
Mkn180	174.1100	70.1576	174.1125	70.1570	3.53	-1.00	-0.81	328.7	3234	2943.5
Mkn180	174.1100	70.1576	174.1128	70.1571	3.51	-1.06	-1.11	328.7	8058	6398.5
ON231	185.3820	28.2329	185.3834	28.2332	4.90	-2.37	0.01	282.6	37	1404.0
ON231	185.3820	28.2329	185.3801	28.2332	3.62	-0.78	-1.02	133.2	660	9899.7
ON231	185.3820	28.2329	185.3798	28.2322	3.59	-0.94	-0.98	108.2	937	8607.0
3C279	194.0465	-5.7893	194.0445	-5.7892	3.52	-1.08	-0.95	121.7	4080	15073.7
3C279	194.0465	-5.7893	194.0445	-5.7893	3.53	-0.87	-0.98	103.8	2673	10655.0
3C279	194.0465	-5.7893	194.0444	-5.7894	3.72	-0.96	-1.13	105.0	351	1587.0
3C279	194.0465	-5.7893	194.0442	-5.7893	3.52	-0.93	-0.83	121.3	5417	19366.3
3C279	194.0465	-5.7893	194.0442	-5.7894	3.52	-0.87	-1.16	120.0	4292	13953.0
3C279	194.0465	-5.7893	194.0442	-5.7894	3.57	-0.91	-1.05	112.5	1143	4129.5
Mkn501	253.4676	39.7602	253.4672	39.7591	3.57	-1.01	-0.63	53.8	1088	546.6
Mkn501	253.4676	39.7602	253.4683	39.7589	3.52	-0.90	0.58	351.7	3856	1835.3
1ES1959+650	299.9994	65.1485	299.9978	65.1469	3.59	-1.27	-0.89	50.1	844	569.1
1ES1959+650	299.9994	65.1485	299.9988	65.1466	3.59	0.17	0.53	49.4	718	325.9
1ES1959+650	299.9994	65.1485	299.9965	65.1457	3.56	-3.12	-0.08	45.8	1128	481.4
1ES1959+650	299.9994	65.1485	299.9988	65.1458	3.52	0.05	-0.77	42.2	3907	1552.0
PKS2005-489	302.3558	-48.8316	302.3550	-48.8326	3.95	-1.55	-0.78	76.2	144	759.2
PKS2005-489	302.3558	-48.8316	302.3548	-48.8319	3.53	-0.90	-1.13	78.6	2857	2794.4
PKS2005-489	302.3558	-48.8316	302.3550	-48.8319	3.51	-1.01	-1.08	79.1	14183	15801.3
PKS2155-304	329.7170	-30.2256	329.7181	-30.2245	3.55	-1.14	-0.46	243.8	1599	937.7
PKS2155-304	329.7170	-30.2256	329.7156	-30.2283	3.51	-0.87	-1.05	52.3	8322	5686.4
PKS2155-304	329.7170	-30.2256	329.7143	-30.2277	3.52	-1.49	-0.73	71.0	4231	2395.3
PKS2155-304	329.7170	-30.2256	329.7148	-30.2280	3.51	-1.16	-0.83	72.2	7564	8096.0
BLLac	330.6804	42.2778	330.6804	42.2760	3.89	-1.01	-0.74	31.3	179	565.1
BLLac	330.6804	42.2778	330.6819	42.2782	3.59	-1.39	-1.13	288.5	921	3447.3
BLLac	330.6804	42.2778	330.6825	42.2781	3.70	-0.90	-0.95	285.8	399	1566.9
BLLac	330.6804	42.2778	330.6819	42.2779	3.60	-1.40	-1.00	281.1	808	2702.8
BLLac	330.6804	42.2778	330.6820	42.2781	3.56	-1.21	-0.72	277.6	1336	4703.5
CTA102	338.1517	11.7308	338.1511	11.7298	3.64	-0.89	-1.19	72.3	560	5257.7
3C454.3	343.4906	16.1482	343.4898	16.1480	3.51	-0.93	-0.95	87.8	13322	13724.1
3C454.3	343.4906	16.1482	343.4898	16.1476	3.51	-0.88	-1.10	75.3	5958	4770.4
1ES2344+514	356.7705	51.7050	356.7685	51.7053	3.54	-0.89	-0.86	136.6	2137	4683.5

Name	RA Optical	Dec Optical	RA XRT	DEC XRT	error	Delta RA	Delta DEC	Roll	Counts	Exposure
1ES2344+514	356.7705	51.7050	356.7687	51.7051	3.55	-0.97	-0.86	101.4	1639	4199.7
1ES2344+514	356.7705	51.7050	356.7726	51.7053	3.52	-0.92	-0.95	273.8	4429	12252.9
1Jy0805-077	122.0647	-7.8528	122.0657	-7.8526	4.05	-0.88	-1.01	296.3	120	5846.9
1Jy0805-077	122.0647	-7.8528	122.0656	-7.8534	3.80	-0.90	-0.88	303.3	252	12955.1
1Jy0805-077	122.0647	-7.8528	122.0636	-7.8535	3.99	-0.46	-1.36	77.3	143	9015.9
1Jy0805-077	122.0647	-7.8528	122.0633	-7.8533	4.51	-0.56	-1.36	84.1	60	3963.5
3C395	285.7331	31.9949	285.7326	31.9948	4.02	-0.57	-1.06	86.5	116	5014.1
1Jy2351+456	358.5903	45.8845	358.5898	45.8844	4.66	-1.06	-1.70	100.4	48	7930.2
1Jy2351+456	358.5903	45.8845	358.5914	45.8828	5.96	0.05	-0.75	35.7	22	1933.0
4U0142+614	26.5934	61.7509	26.5910	61.7513	3.50	-0.97	-1.15	136.0	25698	14721.3
4U0142+614	26.5934	61.7509	26.5900	61.7496	3.66	-0.52	-1.09	78.7	466	238.2
4U0142+614	26.5934	61.7509	26.5899	61.7494	3.53	-0.94	-1.02	77.0	2730	1396.1
1ES0033+595	8.9693	59.8346	8.9684	59.8355	3.52	-1.19	-1.02	177.1	4442	3829.6
1ES0033+595	8.9693	59.8346	8.9674	59.8354	3.52	-0.98	-0.97	154.4	3608	3004.9
1ES0033+595	8.9693	59.8346	8.9681	59.8349	3.51	-0.78	-0.87	117.1	7165	4237.2
AKN564	340.6645	29.7250	340.6617	29.7241	3.51	-1.07	-1.28	102.3	6320	4605.8
AKN564	340.6645	29.7250	340.6630	29.7247	3.51	-0.72	-0.96	78.6	5991	4409.6
AKN564	340.6645	29.7250	340.6656	29.7261	3.51	-0.92	-0.96	256.0	7437	4688.3
PKS0823-223	126.5066	-22.5076	126.5084	-22.5075	4.28	-0.95	-0.95	320.5	89	2908.4
PKS0823-223	126.5066	-22.5076	126.5077	-22.5085	3.64	-0.68	-0.84	329.8	548	20367.9
PKS0823-223	126.5066	-22.5076	126.5074	-22.5088	3.60	-1.14	-0.82	332.5	848	31354.7
PKS0823-223	126.5066	-22.5076	126.5060	-22.5087	3.97	-0.86	-1.24	57.2	139	7374.3
PKS0823-223	126.5066	-22.5076	126.5051	-22.5088	4.11	-1.31	-1.01	82.6	110	5106.9
PKS0823-223	126.5066	-22.5076	126.5051	-22.5092	3.94	-0.62	-0.88	85.9	157	5887.1
PKS0823-223	126.5066	-22.5076	126.5053	-22.5088	3.83	-0.84	-1.34	87.0	225	8938.4
PKS0823-223	126.5066	-22.5076	126.5052	-22.5088	3.70	-0.93	-0.78	86.4	379	16160.2
PKS0823-223	126.5066	-22.5076	126.5051	-22.5081	3.73	-0.94	-1.21	90.1	333	12395.0
PKS0823-223	126.5066	-22.5076	126.5039	-22.5071	4.97	0.26	-0.26	130.6	44	1943.2
PKS0823-223	126.5066	-22.5076	126.5040	-22.5078	3.84	-0.96	-0.75	133.8	211	9815.9
RXJ0148.3-2758	27.0930	-27.9738	27.0934	-27.9747	3.54	-1.05	-0.89	22.2	2028	7667.2
RXJ0148.3-2758	27.0930	-27.9738	27.0931	-27.9747	3.52	-0.98	-1.21	24.2	5664	22053.1
RXJ0148.3-2758	27.0930	-27.9738	27.0931	-27.9749	3.54	-1.22	-1.16	27.1	2105	8874.3
RXJ0148.3-2758	27.0930	-27.9738	27.0928	-27.9748	3.59	-1.24	-1.22	29.1	976	3144.1
RXJ0148.3-2758	27.0930	-27.9738	27.0937	-27.9720	3.79	-1.14	-0.80	217.1	273	824.2
RXJ0148.3-2758	27.0930	-27.9738	27.0936	-27.9719	3.59	-0.83	-0.79	220.8	926	6371.0
RXJ0148.3-2758	27.0930	-27.9738	27.0942	-27.9721	3.72	-0.45	-0.74	227.9	352	5122.4
RXJ0148.3-2758	27.0930	-27.9738	27.0944	-27.9719	3.67	-1.41	-0.81	229.3	481	3520.2
Mkn684	217.7696	28.2869	217.7709	28.2871	3.65	-1.45	-0.95	301.2	527	4758.5
Mkn684	217.7696	28.2869	217.7704	28.2877	3.57	-0.95	-0.77	259.8	1145	12907.5
Mkn684	217.7696	28.2869	217.7712	28.2882	3.57	-0.93	-0.68	252.7	1230	8226.2
Mkn684	217.7696	28.2869	217.7719	28.2862	3.81	-0.95	-0.82	337.1	244	1368.9
Mkn684	217.7696	28.2869	217.7713	28.2861	3.57	-1.20	-1.23	341.5	1281	6564.1
RXJ2216.8-4451	334.2217	-44.8658	334.2202	-44.8659	3.54	-0.78	-1.10	114.5	2396	19020.1
Mkn728	165.2574	11.0468	165.2583	11.0474	3.59	-0.85	-1.18	291.0	946	4488.0
Mkn728	165.2574	11.0468	165.2565	11.0468	3.73	0.57	-0.79	105.8	296	6561.4
Mkn915	339.1938	-12.5452	339.1929	-12.5461	3.87	-1.10	-0.59	78.3	201	2863.3
Mkn915	339.1938	-12.5452	339.1947	-12.5438	3.58	-1.19	-0.74	248.1	1080	11505.9
ESO506-27	189.7267	-27.3078	189.7283	-27.3080	3.91	-0.65	-0.49	285.2	164	7361.4
ESO506-27	189.7267	-27.3078	189.7283	-27.3073	4.78	-1.89	-2.39	308.1	44	2027.9
ESO506-27	189.7267	-27.3078	189.7286	-27.3084	3.83	-1.37	-0.85	315.1	192	10948.5
SS433	287.9565	4.9827	287.9573	4.9815	3.89	-1.16	-0.55	317.2	185	205.6
SS433	287.9565	4.9827	287.9581	4.9812	3.56	-0.53	-0.26	314.2	1208	989.6
SS433	287.9565	4.9827	287.9586	4.9817	3.56	-1.91	-1.90	314.2	1059	1246.1
SS433	287.9565	4.9827	287.9580	4.9827	3.55	-0.94	-0.81	297.4	1594	1269.7
SS433	287.9565	4.9827	287.9566	4.9807	3.56	-0.73	-0.93	33.9	1451	2840.2
SS433	287.9565	4.9827	287.9565	4.9807	3.52	-0.89	-0.80	31.3	4959	7737.7
OW+154.9	308.8430	10.9352	308.8409	10.9337	4.90	-0.81	-0.92	88.6	39	2880.5
OW+154.9	308.8430	10.9352	308.8415	10.9340	5.14	-1.07	-1.56	89.0	36	2030.9
OW+154.9	308.8430	10.9352	308.8417	10.9352	4.16	-0.76	-1.50	95.0	106	5628.7
S52010+72	302.4679	72.4887	302.4614	72.4905	5.76	-1.85	-1.90	143.8	19	3302.1
S52010+72	302.4679	72.4887	302.4623	72.4880	4.83	0.00	-0.51	118.3	31	4795.8
RXJ0720.4-3125	110.1040	-31.4306	110.1041	-31.4297	3.57	-1.17	-1.02	232.9	1203	4001.6
RXJ0720.4-3125	110.1040	-31.4306	110.1049	-31.4309	3.53	-1.14	-0.92	293.2	2702	8508.8
Mrk876	243.4883	65.7194	243.4878	65.7198	3.68	-1.10	-1.27	145.3	443	3783.0
Mrk876	243.4883	65.7194	243.4867	65.7187	3.53	-1.11	-1.02	75.3	3392	25676.5

Name	RA Optical	Dec Optical	RA XRT	DEC XRT	error	Delta RA	Delta DEC	Roll	Counts	Exposure
Mrk876	243.4883	65.7194	243.4865	65.7188	3.53	-0.82	-1.11	70.4	3491	23279.0
Mrk876	243.4883	65.7194	243.4865	65.7187	3.56	-0.69	-0.72	68.5	1403	9438.8
H1426+428	217.1354	42.6736	217.1374	42.6719	3.50	-0.98	-0.78	319.4	28768	21460.6
H1426+428	217.1354	42.6736	217.1374	42.6723	3.50	-1.02	-0.75	314.8	24425	22908.6
PSR0540-69	85.0322	-69.3348	85.0489	-69.3319	3.52	-2.55	-0.59	296.7	3553	8440.8
PSR0540-69	85.0322	-69.3348	85.0485	-69.3323	3.54	-2.55	-0.90	304.6	1536	3318.9
PSR0540-69	85.0322	-69.3348	85.0488	-69.3321	3.52	-1.13	-1.03	305.6	3027	6644.3
PSR0540-69	85.0322	-69.3348	85.0488	-69.3321	3.52	-1.50	-0.80	313.3	3439	7339.5
PSR0540-69	85.0322	-69.3348	85.0485	-69.3324	3.52	-1.00	-0.52	319.1	3623	8071.4
3C279	194.0465	-5.7893	194.0490	-5.7889	4.22	-1.33	-0.95	299.1	101	265.8
3C279	194.0465	-5.7893	194.0487	-5.7891	3.83	-1.08	-1.15	299.0	233	575.9
3C279	194.0465	-5.7893	194.0478	-5.7897	4.06	-0.97	-0.59	298.1	129	387.7
3C279	194.0465	-5.7893	194.0477	-5.7887	3.88	-1.15	-0.67	298.1	186	573.8
3C279	194.0465	-5.7893	194.0490	-5.7895	3.98	-0.95	-0.94	298.2	148	387.8
3C279	194.0465	-5.7893	194.0488	-5.7894	3.85	-0.85	-0.72	298.3	204	569.2
3C279	194.0465	-5.7893	194.0487	-5.7898	4.07	-1.52	-0.64	298.0	124	385.0
3C279	194.0465	-5.7893	194.0486	-5.7895	4.00	-1.00	-0.79	298.1	141	430.9
3C279	194.0465	-5.7893	194.0486	-5.7890	4.08	-1.17	-0.72	284.4	125	390.9
3C279	194.0465	-5.7893	194.0483	-5.7892	3.83	-1.22	-1.00	284.4	227	569.2
3C279	194.0465	-5.7893	194.0485	-5.7886	4.37	-0.81	-0.72	284.7	75	277.7
3C279	194.0465	-5.7893	194.0485	-5.7885	3.71	-1.15	-1.48	284.7	166	575.9
3C279	194.0465	-5.7893	194.0486	-5.7891	4.39	-1.49	-1.17	284.3	79	263.1
3C279	194.0465	-5.7893	194.0486	-5.7885	4.28	-0.45	-0.62	284.3	91	288.9
3C279	194.0465	-5.7893	194.0482	-5.7885	4.10	-1.42	-0.61	284.2	116	378.6
3C279	194.0465	-5.7893	194.0488	-5.7888	3.98	-1.28	-0.78	284.2	146	506.4
3C279	194.0465	-5.7893	194.0480	-5.7894	4.12	-0.98	-1.08	284.9	116	383.6
3C279	194.0465	-5.7893	194.0483	-5.7890	4.02	-1.14	-0.70	284.9	140	408.5
3C279	194.0465	-5.7893	194.0493	-5.7895	4.24	-0.44	-0.64	285.6	89	222.9
3C279	194.0465	-5.7893	194.0484	-5.7895	4.17	-0.89	-1.36	285.6	101	283.9
3C279	194.0465	-5.7893	194.0494	-5.7894	4.59	-1.17	-1.78	284.3	57	282.9
3C279	194.0465	-5.7893	194.0487	-5.7897	4.49	-1.32	-0.54	284.0	69	220.2
3C279	194.0465	-5.7893	194.0488	-5.7887	4.38	-0.13	-0.40	285.1	74	222.5
3C279	194.0465	-5.7893	194.0485	-5.7891	4.40	-0.75	-0.48	284.8	69	230.2
3C279	194.0465	-5.7893	194.0484	-5.7884	4.44	-1.76	-1.59	284.4	69	230.2
3C279	194.0465	-5.7893	194.0485	-5.7884	3.95	-1.12	-1.50	285.4	72	245.3
3C279	194.0465	-5.7893	194.0481	-5.7887	4.10	-0.56	-0.81	284.6	122	333.5
3C279	194.0465	-5.7893	194.0481	-5.7887	3.88	-1.10	-0.80	284.7	198	569.1
3C279	194.0465	-5.7893	194.0479	-5.7891	4.26	-0.44	-0.84	285.4	85	265.8
3C279	194.0465	-5.7893	194.0488	-5.7888	3.86	-1.09	-1.09	285.5	197	575.9
3C279	194.0465	-5.7893	194.0482	-5.7889	4.34	-1.60	-0.70	284.6	81	273.3
3C279	194.0465	-5.7893	194.0489	-5.7890	3.84	-0.98	-1.18	284.7	214	574.2
3C279	194.0465	-5.7893	194.0484	-5.7893	4.22	-0.84	-1.24	285.2	96	273.3
3C279	194.0465	-5.7893	194.0487	-5.7886	3.88	-1.71	-1.31	285.2	192	575.9
3C279	194.0465	-5.7893	194.0488	-5.7880	4.19	-1.49	-1.81	284.3	100	277.9
3C279	194.0465	-5.7893	194.0485	-5.7897	4.22	-1.77	-0.94	299.4	94	284.9
3C279	194.0465	-5.7893	194.0484	-5.7896	3.91	-0.97	-1.68	299.4	184	575.9
3C279	194.0465	-5.7893	194.0478	-5.7888	4.15	-1.81	-1.41	298.1	103	323.4
3C279	194.0465	-5.7893	194.0487	-5.7888	3.86	-1.08	-1.14	298.1	203	575.9
3C279	194.0465	-5.7893	194.0485	-5.7895	4.10	-1.53	-0.97	295.5	120	323.4
3C279	194.0465	-5.7893	194.0488	-5.7896	3.95	-1.04	-1.14	295.5	153	575.9
3C279	194.0465	-5.7893	194.0483	-5.7894	4.10	-1.21	-0.71	299.3	117	325.9
3C279	194.0465	-5.7893	194.0483	-5.7890	3.85	-1.10	-0.47	299.3	228	575.9
3C279	194.0465	-5.7893	194.0484	-5.7879	4.16	-1.33	-0.88	298.7	105	398.7
3C279	194.0465	-5.7893	194.0492	-5.7891	4.02	-1.30	-1.00	298.8	129	574.9
3C279	194.0465	-5.7893	194.0499	-5.7891	4.07	-0.30	-0.89	298.2	110	396.1
3C279	194.0465	-5.7893	194.0492	-5.7886	3.96	-1.88	-1.14	298.2	160	575.9
GD153	194.2597	22.0313	194.2596	22.0297	5.64	-0.95	0.09	38.1	24	2524.3
GD153	194.2597	22.0313	194.2612	22.0336	12.15	1.33	-0.33	268.8	3	1299.1
GD153	194.2597	22.0313	194.2580	22.0313	6.04	-1.03	-1.69	130.4	21	2946.0
RXJ0117.5-3826	19.3778	-38.4416	19.3776	-38.4423	3.78	-0.54	-1.24	38.7	269	3555.2
RXJ0117.5-3826	19.3778	-38.4416	19.3768	-38.4409	4.00	-0.66	-0.76	165.5	136	3365.3
RXJ0117.5-3826	19.3778	-38.4416	19.3762	-38.4404	3.75	-1.08	-0.67	168.3	313	3440.0
Burst	100.1971	-37.0729	100.1969	-37.0726	3.65	-0.76	-1.04	172.2	556	3892.2
GRB050219b	81.3166	-57.7580	81.3191	-57.7573	6.78	-0.98	-1.00	275.8	3	9052.0
GRB050315	306.4754	-42.6006	306.4745	-42.6009	3.53	-0.97	-1.05	61.2	2350	13517.6

Name	RA Optical	Dec Optical	RA XRT	DEC XRT	error	Delta RA	Delta DEC	Roll	Counts	Exposure
GRB050318	49.7125	-46.3956	49.7134	-46.3959	3.55	-1.38	-1.19	299.6	1764	23524.3
GRB050319	154.1996	43.5485	154.2006	43.5480	3.55	-1.01	-1.23	325.9	1794	13064.4
GRB050401	247.8700	2.1873	247.8691	2.1868	3.58	-0.82	-0.99	82.9	985	2356.1
GRB050406	34.4679	-50.1875	34.4699	-50.1884	3.82	-0.66	-1.23	338.1	160	49528.2
GRB050416a	188.4775	21.0574	188.4786	21.0569	3.55	-0.92	-1.10	331.5	1820	57215.2
GRB050505	141.7638	30.2733	141.7647	30.2731	3.52	-1.22	-0.82	288.6	4488	57286.0
GRB050525	278.1358	26.3399	278.1355	26.3381	3.63	-0.81	-0.91	40.1	601	5757.7
GRB050607	300.1783	9.1421	300.1776	9.1408	3.57	-1.11	-0.99	53.1	1114	7848.0
GRB050712	77.7004	64.9132	77.6974	64.9138	3.60	-0.94	-0.99	135.7	799	5347.4
GRB050713a	320.5400	77.0747	320.5404	77.0735	3.58	-0.96	-1.16	26.2	989	4011.4
GRB050721	253.4355	-28.3811	253.4371	-28.3808	3.57	-1.23	-1.11	270.4	1212	1303.1
GRB050724	246.1849	-27.5410	246.1873	-27.5401	3.63	-1.26	-1.10	274.9	563	25834.9
GRB050730	212.0714	-3.7716	212.0730	-3.7719	3.51	-1.11	-0.91	288.9	11565	58479.6
GRB050801	204.1475	-21.9283	204.1491	-21.9285	3.62	-1.46	-0.97	293.5	596	23117.0
GRB050802	219.2737	27.7867	219.2757	27.7865	3.52	-1.13	-1.10	284.3	4938	43571.0
GRB050814	264.1891	46.3393	264.1910	46.3393	3.56	-0.88	-0.90	301.8	1296	44328.0
GRB050815	293.5965	9.1465	293.5968	9.1470	3.80	-1.16	-1.15	305.8	255	6356.0
GRB050820a	337.4088	19.5603	337.4092	19.5586	3.51	-0.91	-0.96	14.2	7436	22136.2
GRB050826	87.7566	-2.6432	87.7553	-2.6449	3.63	-1.41	-0.90	77.7	530	56943.2
GRB050904	13.7117	14.0861	13.7111	14.0847	3.51	-1.02	-0.83	56.8	6279	22225.0
GRB050908	20.4613	-12.9544	20.4598	-12.9555	3.61	-1.16	-0.88	99.3	708	19817.6
GRB050915	81.6868	-28.0165	81.6855	-28.0172	3.65	-0.99	-1.15	88.5	527	10628.3
GRB050922C	317.3879	-8.7583	317.3890	-8.7576	3.55	-1.14	-0.95	260.6	1479	23109.6
GRB051109a	330.3138	40.8231	330.3152	40.8235	3.53	-0.86	-0.77	267.1	2944	10139.8
GRB051221	328.7028	16.8908	328.7036	16.8921	3.59	-0.71	-0.92	236.8	915	26879.9
GRB051227	125.2423	31.9255	125.2405	31.9244	3.77	-0.25	-0.73	78.3	259	3390.2
GRB060111B	286.4270	70.3759	286.4238	70.3778	3.60	-1.05	-1.01	173.6	728	30017.1
GRB060115	54.0350	17.3453	54.0361	17.3466	3.60	-1.47	-0.91	255.3	833	3788.2
GRB060203	103.5160	71.8107	103.5222	71.8103	3.63	-1.08	-1.56	321.3	617	22891.6
GRB060204b	211.8121	27.6768	211.8102	27.6759	3.56	-0.98	-1.01	97.4	1451	7754.7
GRB060206	202.9311	35.0509	202.9285	35.0496	3.77	-1.13	-0.79	88.1	262	1188.6
GRB060210	57.7392	27.0262	57.7404	27.0275	3.52	-1.13	-0.94	258.8	5962	23135.8
GRB060218	50.4155	16.8674	50.4168	16.8682	3.55	-0.99	-0.99	255.5	1501	52854.4
GRB060223	55.2065	-17.1301	55.2118	-17.1264	7.97	5.75	-2.25	271.0	3	8700.0
GRB060323	174.4385	49.9854	174.4400	49.9838	3.84	-1.20	-0.91	349.5	216	8756.9
GRB060418	236.4275	-3.6389	236.4258	-3.6405	3.58	-1.16	-0.65	75.0	936	2368.3
GRB060428a	123.5450	-37.1698	123.5472	-37.1694	3.55	-1.22	-1.09	282.3	1598	9228.3
GRB060428b	235.3568	62.0251	235.3581	62.0227	3.62	-0.86	-1.16	19.6	633	11034.5
GRB060502	240.9270	66.6007	240.9288	66.5980	3.59	-0.62	-1.16	21.0	836	2776.5
GRB060505	331.7643	-27.8144	331.7622	-27.8165	4.32	-0.55	-1.36	75.4	66	7750.4
GRB060507	89.9605	75.2489	89.9647	75.2504	3.61	-0.86	-0.81	230.3	692	22749.1
GRB060510a	95.8666	-1.1628	95.8678	-1.1622	3.53	-0.81	-0.48	293.7	2624	1822.8
GRB060510b	239.1234	78.5703	239.1252	78.5683	3.62	-0.77	-1.23	11.5	637	7810.3
GRB060512	195.7742	41.1908	195.7760	41.1895	3.58	-0.72	-0.92	325.0	905	59489.7
GRB060522	322.9367	2.8862	322.9362	2.8848	3.65	-0.69	-0.81	69.3	504	10421.7
GRB060526	232.8263	0.2844	232.8274	0.2838	3.60	-0.99	-1.01	335.0	795	3966.0
GRB060604	337.2292	-10.9155	337.2278	-10.9174	3.62	-0.86	-0.58	68.7	667	28782.6
GRB060605	322.1555	-6.0587	322.1539	-6.0603	3.55	-0.80	-0.98	68.1	1700	30690.9
GRB060607	329.7100	-22.4963	329.7075	-22.4992	3.51	-1.35	-1.27	73.5	6835	21335.5
GRB060614	320.8839	-53.0267	320.8809	-53.0276	3.56	-0.48	-1.06	100.9	1286	10758.0
GRB060707	357.0792	-17.9047	357.0779	-17.9066	3.58	-0.82	-1.22	72.8	971	3118.4
GRB060708	7.8076	-33.7590	7.8050	-33.7602	3.63	-0.81	-1.23	75.8	618	2685.2
GRB060714	227.8602	-6.5662	227.8626	-6.5660	3.60	-0.86	-1.14	290.9	793	1559.5
GRB060719	18.4320	-48.3809	18.4297	-48.3826	3.59	-1.06	-0.84	82.8	837	17486.0
GRB060729	95.3827	-62.3702	95.3815	-62.3722	3.54	-0.70	-1.41	31.7	1959	4851.0
GRB060804	112.2057	-27.2158	112.2056	-27.2176	3.60	-1.10	-0.87	28.2	786	11962.2
GRB060904B	58.2105	-0.7252	58.2083	-0.7264	3.60	-1.21	-0.88	82.7	739	15581.1
GRB060908	31.8265	0.3420	31.8245	0.3405	3.55	-0.94	-0.99	81.6	1473	3391.7
GRB060912	5.2840	20.9716	5.2840	20.9698	3.59	-0.85	-1.29	31.7	873	6814.2
GRB060923c	346.1180	3.9247	346.1203	3.9268	5.40	-0.64	-2.73	246.8	18	8807.5

5. References

Hill, J.E., *et al*., "The unique operating modes of the Swift X-ray Telescope", 2005, Proc. SPIE, 5898, 313
Moretti, A., *et al*., "A refined position catalog of the Swift XRT afterglows", 2006, Astronomy & Astrophysics, 448, L9
Burrows, D.N., *et al*, GCN Circular 5750, 2006
Kennea, J.A., *et al*, GCN 5872, 2006